Chemical Science

EDGE ARTICLE

View Article Online
View Journal | View Issue

Cite this: *Chem. Sci.*, 2014, **5**, 3425

Structure determined charge transport in single DNA molecule break junctions†

Kun Wang,[a] Joseph M. Hamill,[a] Bin Wang,[a] Cunlan Guo,[a] Sibo Jiang,[b] Zhen Huang[b] and Bingqian Xu*[a]

Received 25th March 2014
Accepted 4th May 2014

DOI: 10.1039/c4sc00888j

www.rsc.org/chemicalscience

Experimental study of the charge transport properties associated with structural variations due to a change in the ionic environment will provide essential physical information in determining the nature of DNA molecules. This work reports an experimental study of the change in electronic transport properties induced by the conformational transition of a poly d(GC)$_4$ DNA. By gradually increasing the concentration of $MgCl_2$ in the buffer solution from 0 M to 4 M, the conductance of the single DNA molecule decreased by two orders of magnitude. Circular dichroism (CD) measurements confirmed that a B to Z conformational transition caused the reduction in conductance. Using a stretch-hold mode scanning probe microscopy break junction (SPMBJ) technique, this B–Z transition process was monitored and a transition trend line was successfully achieved from conductance measurements alone. The transition midpoint occurred at a $MgCl_2$ concentration of 0.93 M for this DNA sequence. This method provides a general tool to study transitions of molecular properties associated with conductance differences.

Introduction

DNA, the repository of genetic information, has gained considerable attention because of its potential application in tomorrow's molecular electronics, such as building DNA chips.[1,2] To pave the way towards this goal, great efforts have been made experimentally and theoretically.[3,4] In order to approximate natural conditions, experiments are usually performed in an appropriate buffer. However, discrepancies exist, not only between experimental results and simulated data, but also among different experimental studies on similar DNA molecules. For example, a wide range of electronic properties of λ-DNA, varying from insulating to conducting and even to superconducting, have been reported by different groups.[5–8] Similarly, for the same DNA, the conductance measured in solution was an order of magnitude greater than the conductance measured in dry conditions.[7] As various simulations suggested, it is quite possible that these discrepancies are caused by different experimental conditions, especially different ionic environments in buffer solutions where the electronic properties of DNA were measured.[9–11] Ions surrounding DNA molecules could not only vary the degree of charge delocalization, but also perturb the structure of DNA molecules.

DNA molecules have proven to exhibit surprising conformational versatility, while retaining remarkable precision and uniformity.[12] As well as right handed (RH) B- and A-DNA, left-handed (LH) Z-DNA has also been explored by chemists and biologists due to its biological and medical significance.[13–15] Using circular dichroism (CD), the ionic conditions necessary to induce a conformation shift from a right-handed (RH) B-DNA to a left-handed (LH) Z-DNA helix have been determined for various counterions.[16–18] The presence of ethanol in addition to alkaline metal ions in solution was also reported to cause a RH internal switch from B- to A-DNA.[19,20]

The conductance of short strands of RH double helix DNA has been determined theoretically and experimentally.[4,21] Concurrent simulations highlighted the conductance changes due to conformational perturbations.[22,23] The dependency of these conformational perturbations on salt concentration suggests that counterion configurations around DNA play a prominent role in charge migration, especially in solutions with high salt concentration.[3,9,10,24–26] Therefore, the ionic environment around DNA has a significant influence on electrical measurements, but this information is unfortunately still missing. Systematic investigations into the correlations between the ionic conditions in buffer solutions and the subsequent physical conformational alteration induced

[a]*Single Molecule Study Laboratory, College of Engineering and Nanoscale Science and Engineering Center, University of Georgia, Athens, GA 30602, USA. E-mail: bxu@engr.uga.edu*

[b]*Department of Chemistry, Georgia State University, Atlanta, GA 30303, USA*

† Electronic supplementary information (ESI) available: Electrical measurement details for log-scale and linear-scale setup, details about DNA structure simulation and 2DCH, results of control experiment conducted in pure 4 M $MgCl_2$ solution with no DNA molecule, estimation of numbers of Mg^{2+} ions around DNA in buffer solution and TD, and pH values and specific TD results at each concentration. See DOI: 10.1039/c4sc00888j

conductance changes of DNA will provide further understanding of the nature of DNA, as well as providing essential groundwork for the development of DNA-based molecular devices.

Given that previous DNA conductance measurements were performed in buffer solutions containing fixed ionic concentrations, it is still unclear how the electronic properties of a short DNA molecule vary as the ionic environment changes, and what the underlying mechanism could be. Herein, we report conductance measurements of poly $d(GC)_4$ DNA based on a SPM break junction (SPMBJ) technique (Fig. 1). By gradually increasing the $MgCl_2$ concentration in the buffer solution, a decrease in conductance by two orders of magnitude was revealed. Circular dichroism (CD) measurements proved the reduction in the charge transport ability of short strand DNA to be a result of a secondary molecular structural transition. Combined with CD, we further developed a novel method to determine the transition degree (TD) and conductance simultaneously.

Results and discussion

Under a constant bias voltage of 0.3 V, the static conductance of poly $d(GC)_4$ DNA was measured in buffer solutions with various $MgCl_2$ concentrations (0 M, 0.1 M, 0.5 M, 1 M, 1.5 M, 2 M, 3 M and 4 M). The 3′ end of single strand DNA was modified with a thiol group in order to form a bond with the Au electrodes to form the molecular junctions. The DNA sample solution prepared at each $MgCl_2$ concentration was dropped on freshly flamed Au(111) to form a DNA monolayer after 40 minutes of incubation. Molecular junctions were formed when the scanning tunneling microscope (STM) tip approached the Au surface, and then broke when the STM tip was retracted from the surface. During each tip retraction process, a conductance trace was recorded. By repeating this process, around 1000 conductance traces were collected for the construction of the final conductance histogram at each $MgCl_2$ concentration. All measurements were conducted at room temperature (~23 °C). More experimental details are provided in Section S1 (see ESI†). A continuous-stretch mode (CSM) SPMBJ was performed for transient Au–DNA–Au junctions by retracting the tip continuously,[27] and a stretch-hold mode (SHM) SPMBJ was applied to create stable junctions by modifying the tip retraction process with a periodic pause.[28]

A logarithmic-scale STM scanner was first applied under CSM to monitor a broad range for a first glance at the possible conductance sets of poly $d(GC)_4$ DNA in 1 M $MgCl_2$ buffer solution, which is supposed to simultaneously access various DNA conformations. In addition to the sharp peaks at integer multiples of the conductance quantum G_0, which correspond to the gold quantum contacts, the histogram also exhibited two apparent peaks at lower conductance: at around 1×10^{-5} G_0 and 1×10^{-3} G_0, respectively (Fig. 2). Representative log-scale conductance traces are shown in Fig. 2B. Previous measurements on the same DNA sequence confirmed the peak at 1×10^{-3} G_0 to be the conductance in a standard double helix B-conformation.[21] Log-scale data offered a complete view of the possible locations of conductance peaks, but failed to provide the highest resolution of details which is necessary for electrical measurements at the single-molecule level. In order to accurately determine the conductance value and gain more details of the DNA molecular junction, a linear-scale STM scanner was then used for a series of different $MgCl_2$ concentrations under both CSM- and SHM-SPMBJ. To measure the conductance at $\sim 1 \times 10^{-3}$ G_0, we chose the measurement window in the higher

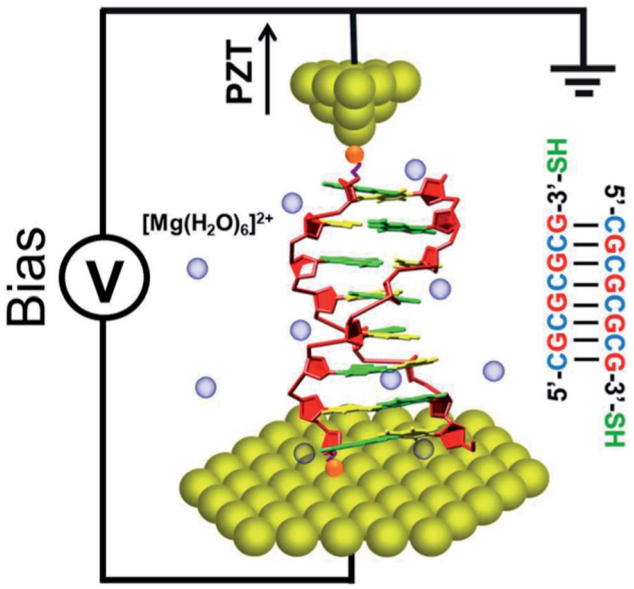

Fig. 1 Experimental schematic of the SPM break junction. $[Mg(H_2O)_6]^{2+}$ ions are represented by spheres around the DNA skeleton. The three hydrogen bonds connecting cytosine and guanine are not shown in the DNA structure.

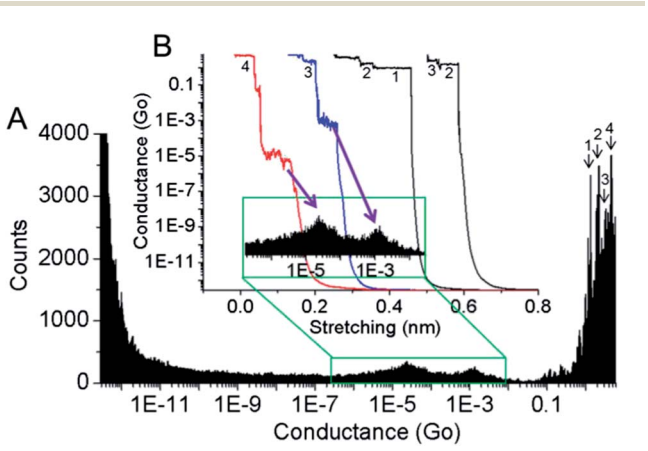

Fig. 2 Log-scale conductance measurements were performed in 1 M $MgCl_2$ solution using CSM-SPMBJ. (A) A log-scale conductance histogram constructed from around 1000 log-scale traces under CSM. (B) Typical conductance traces are shown. The left two traces exhibited plateaus corresponding to peaks at around 1×10^{-5} G_0 and 1×10^{-3} G_0, respectively. The numbers labelled in the conductance histograms and traces represent integer multiples of the conductance quantum G_0. The inset in B shows the enlarged view of the selected area in the log-scale conductance histogram.

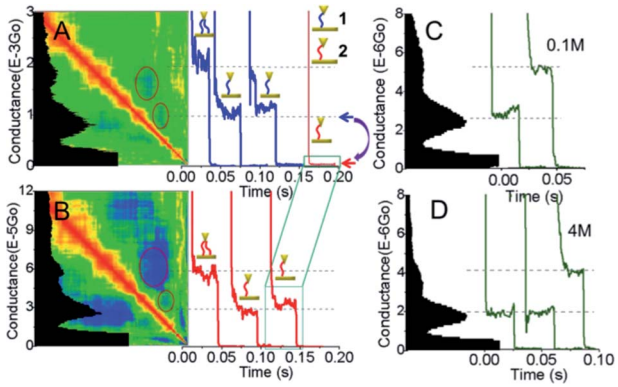

Fig. 3 (A) and (B) show the conductance measurement results of poly $d(GC)_4$ DNA. In 1 M $MgCl_2$ solution, two sets of conductance values (1×10^{-3} G_0 in A and 1×10^{-5} G_0 in B) were determined by conductance histograms using the measured conductance traces. In A and B, the rough schematics (1 and 2) of DNA molecular junctions are shown above the each conductance plateau. Short curved strands in blue and red represent the DNA molecules with high and low conductance, respectively. The number of short curved strands in each schematic represents how many DNA molecules were measured when the plateau was recorded. The 2DCH shows strong anti-correlation regions (circled in 2DCH). For 5′-CGCGAAACGCG-3′DNA, SHM conductance histograms and typical conductance traces measured at 0.1 M and 4 M are shown in panels (C) and (D), respectively.

conductance region (Fig. 3A). As is shown in Fig. 3A, a representative conductance trace (the furthest right) contains a very low plateau at the same level of baseline offset shift. Unfortunately, this information was entirely washed out by slight shifting of the conductance trace baseline under this window. To reveal the lower conductance plateau, we measured the conductance curves by focusing on the lower conductance region, which shows a conductance of $\sim 3 \times 10^{-5}$ G_0 (Fig. 3B). Therefore, using SHM-SPMBJ measurements, the two peaks were accurately measured to be $1.06 (\pm 0.27) \times 10^{-3}$ G_0 and $2.79 (\pm 0.64) \times 10^{-5}$ G_0 in 1 M $MgCl_2$ solution, respectively. We then measured the conductance of the poly $d(GC)_4$ DNA under different $MgCl_2$ concentrations. For lower concentrations (0 M, 0.1 M, 0.5 M), a conductance peak around 1×10^{-3} G_0 was measured, suggesting the DNA to be B-DNA. However for medium and high concentrations (1–4 M), a larger number of individual conductance traces appeared to have significant information at a much lower conductance value, which was associated with the peak at around 1×10^{-5} G_0 under log scale. Control experiments conducted in pure 4 M $MgCl_2$ solution with no DNA imply that these peaks were mostly contributed by DNA molecules, rather than other factors such as counter ions and water molecules in the solution (Fig. S2a, see ESI†). A two-dimensional correlation histogram (2DCH) was also demonstrated for the two measurement regions (Section S3, see ESI†). Strong anti-correlation regions (circled areas in Fig. 3) suggest the possibility that each conductance trace contained only a single conductance plateau, at the height of either one or two Au–DNA–Au junctions, but rarely both together.

While the 1×10^{-3} G_0 conductance value was reported to be associated with B-DNA, the appearance of the conductance peak at the level of 1×10^{-5} G_0 could be attributed to several possible causes. Firstly, both base pair (bp) mismatch and the single strand DNA could be the source. As poly $d(GC)_4$ is the chosen sequence, there would be multiple mismatched bps once the bp mismatch took place. However, even the mismatch of a single bp leads to a decrease in conductance by one order of magnitude, so multiple mismatches will make the DNA nearly insulating,[29] which suggests the impossibility of observing the conductance of mismatched DNA molecules. Also, in our case, single strand DNA was hardly present due to the high melting temperature (>50 °C) of DNA molecules in 1 M $MgCl_2$ solution. Even if it existed, the single strand DNA could not form the molecular junction since only one end of the single strand was modified with a thiol group. Thus, the peak at the level of 1×10^{-5} G_0 did not result from single strand DNA or bp mismatch. Secondly, as many studies have reported, variations in Au–S geometries, effective contact coupling and the DNA solvation shell could also cause a decrease in conductance by orders of magnitude.[30–33] To find out if these factors caused the conductance drop, another series of control experiments were conducted on the DNA sequence of 5′-CGCGAAACGCG-3′, which has little perturbation in structure due to the three consecutive adenine bases sandwiched at the center of the sequence.[34,35] The CD results in Fig. 4C suggest that this DNA still remained in the RH B-conformation, even after the addition of high concentrations of $MgCl_2$. Under SHM, conductance of this DNA sequence was measured in $MgCl_2$ solutions prepared in the same way as for poly $d(GC)_4$ DNA. As shown in Fig. 3C and D, the conductance showed only a negligible variation, from around 2.5×10^{-6} G_0 in 0.1 M $MgCl_2$ solution to 2.0×10^{-6} G_0 in 4 M $MgCl_2$ solution. This small change could possibly be caused by the slight structural perturbation of DNA in solutions with high $MgCl_2$ concentration, confirmed by the CD measurements (Fig. 4C). An insignificant number of conductance traces containing low but meaningful plateaus, like in the case of poly $d(GC)_4$ DNA, were observed with $MgCl_2$ concentrations spanning from 0 M to 4 M in the control measurements. Overall, both conductance measurements and CD results suggest that the influence of contact geometries, effective coupling and the solvation shell were trivial in this study. Finally, the newly revealed peak, two orders of magnitude smaller in conductance, could be contributed by another conformation of the poly $d(GC)_4$ DNA duplex.

Over a series of measurements, it was determined that the histogram peak at $1.06 (\pm 0.27) \times 10^{-3}$ G_0 did not show an obvious change with small increases in Mg^{2+} concentration from 0 M, 0.1 M and 0.5 M, or even over the entire range of concentrations from 0 M to 4 M. Instead, the magnitude of this peak decreased with increasing Mg^{2+} concentration, while the magnitude of the other peak at $2.79 (\pm 0.64) \times 10^{-5}$ G_0 became more pronounced. This implies a clear ratio switch between these two peaks as Mg^{2+} concentration increases. The change by two orders of magnitude suggests, not a linear relationship between DNA conductance and counter ion concentration, but a

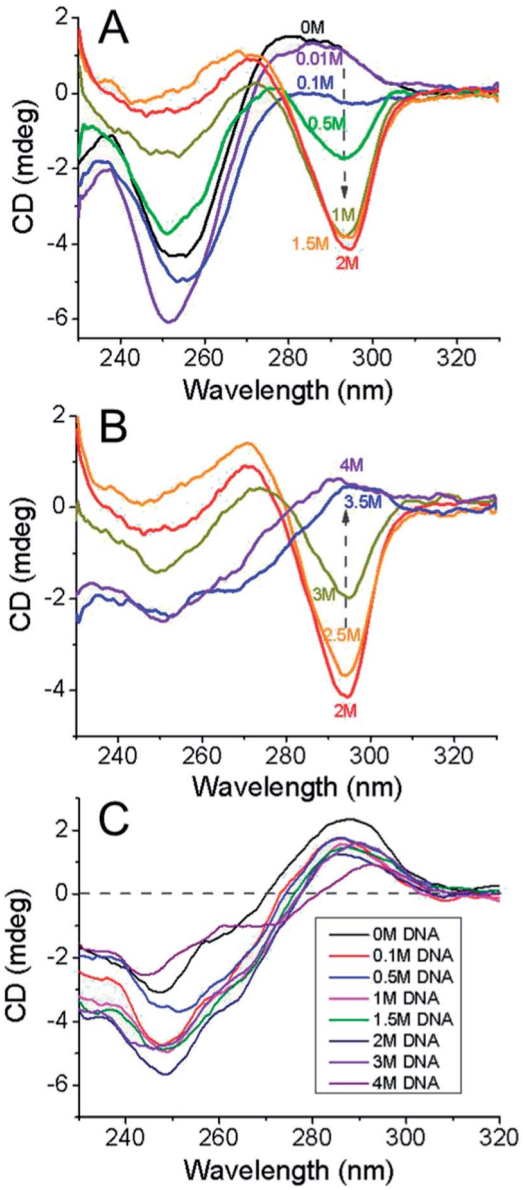

Fig. 4 (A) and (B) show the CD spectra of poly d(GC)$_4$ DNA measured in 0–2 M and 2–4 M $MgCl_2$ solutions, respectively. The arrow in both panels indicates the trend of change in CD intensity at 295 nm as the $MgCl_2$ concentration increases. Panel (C) shows the CD spectra of 5′-CGCGAAACGCG-3′DNA measured in 0–4 M $MgCl_2$ solutions.

significant regime change such as a compete change in DNA conformation.

A likely explanation is a change from RH B-DNA to LH Z-DNA, which can be tested by CD measurements, since CD studies[16,36] have thoroughly explored the ion-dependent transition between B- and Z-DNA. Therefore, we conducted CD measurements on DNA samples under the same $MgCl_2$ concentrations as the conductance measurements, and also two additional concentrations of 0.01 M and 3.5 M. Fig. 4A (concentrations from 0 M to 2 M) shows the complete transition from B-DNA spectra (a positive peak at 275 nm and a negative peak at 250 nm) to Z-DNA spectra (a negative peak at 295 nm and a positive peak at 265 nm), similar to other reports.[16,36,37] An unexpected inconsistency in CD trend was observed in concentrations beyond 2 M (Fig. 4B). Negative peaks of increasingly lower intensity were observed at 295 nm, until the peaks eventually became a small bump at very high $MgCl_2$ concentrations (3.5 M and 4 M). We suggest that aggregation of individual DNA molecules was the cause of this odd trend at very high $MgCl_2$ concentrations (3.5 M, 4 M), because high Mg^{2+} concentrations can readily induce the aggregation of short DNA molecules, and the spectra at 3.5 M and 4 M resemble curves associated with ψ-form DNA condensations.[38–41]

To confirm this, STM imaging was carried out on samples prepared in the same way as for CD measurements (Fig. 5). At 0.1 M, a well-assembled monolayer of DNA molecules was observed. After drying the solution with high purity nitrogen, imaging in air showed a negligible aggregation spot in only one of a few images, which may be due to the high concentration (5 μM) of DNA molecules. In 4 M $MgCl_2$ solution, imaging in solution showed lots of aggregation spots in all images. The imaging in air showed even more aggregation spots, because drying the sample forced floating aggregation bundles which could not be seen in solution to attach to the surface. More STM images are provided in Fig. S1 (see ESI†). A control experiment conducted in pure 4 M $MgCl_2$ solution with no DNA molecules revealed no aggregation spots *via* both imaging in solution and in air, which excludes the possibility that these spots were induced by condensation of salt (Fig. S2B and S2C, see ESI†).

It has to be noted that the buffer pH decreased as the $MgCl_2$ concentration increased (Table S3†). Previous CD studies using the same DNA sequence proved that low pH (<3.6) could also contribute to the B–Z conformational transition.[42,43] Therefore,

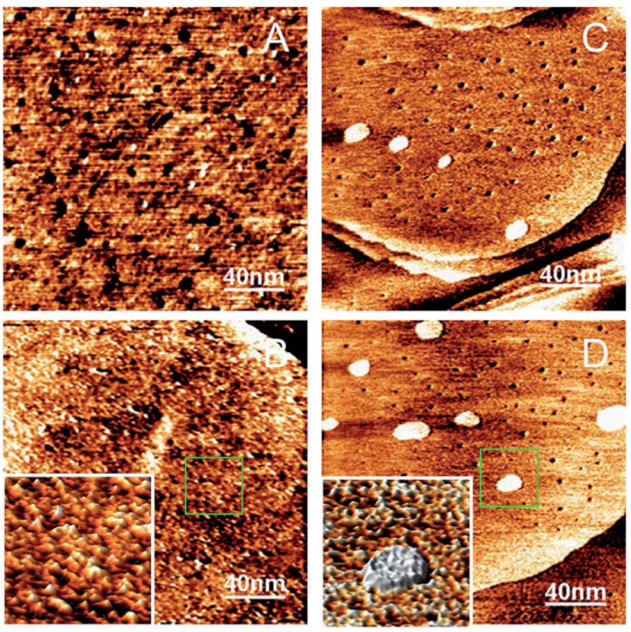

Fig. 5 STM imaging for DNA samples in 0.1 M ((A) and (C)) and 4 M ((B) and (D)). Panels (A) and (B) are images scanned in solution under 0.1 M and 4 M, respectively. Panels (C) and (D) show images obtained in air under 0.1 M and 4 M, respectively.

other than the high ionic concentration, the low pH of the buffer solution is another factor inducing the B–Z transition when the $MgCl_2$ concentration was high (>3 M). The exact concentration of $MgCl_2$ dissolved in buffer solution decreased as the buffer pH reduced. Given that it is hard to know the exact concentration, we continue using the concentration labelled when we prepared the solution in the following discussion.

Due to DNA aggregation, CD failed to distinguish Z-DNA at high $MgCl_2$ concentrations; however the conductance measurement has little difficulty handling aggregation because STM can image prior to conductance measurements. Before measuring, smooth locations indicative of a DNA monolayer on the Au surface were chosen to conduct measurements. The Au surface itself contributed to breaking up aggregates, and any aggregates floating in solution would not have influenced the conductance measurements, and certainly would not have contributed to histogram peaks.

The cause of conductance decrease from B- to Z-DNA

The cause of the decrease in DNA conductance during B–Z conformational transition may come from a few sources, but is primarily due to the structural change induced breaking of π–π orbital stacking between neighboring bps. In Fig. 6A, the average rise (d) between adjacent bps was increased by 14% from 0.332 nm (in B-DNA) to 0.380 nm (in Z-DNA), which could rapidly reduce the charge transfer rate; the axial twist (β) in Z-DNA was determined to be −30°, which is very different from the 36° angle for the highest charge transport in B-DNA. Most importantly, the transition results in a flipping of guanine (G) bases by almost 180° for this DNA sequence (Fig. 6B).[23] The alternating *anti* and *syn* orientations transform the location of G bases from the center of the helix in B-DNA to the edge of the helix in Z-DNA. These changes cause the bases to be held on the edge of the helix, and place guanine bases over the neighboring cytosine's sugar residues. The result is a disruption of the ordered π–π stacking, which is the major source of the relatively high conductance of B-DNA (Fig. 6C and D).[3,44] Although the diameter of Z-DNA is narrower, charge transport along neighboring bps is much easier longitudinally than laterally, and the broken stacking, increased rise and spiral intra-strand path result in a significant reduction in conductance on going from B- to Z-DNA.[45] Since the HOMO is dominated by G orbitals in sequences such as this,[4] the flipping of G will have a detrimental effect on distribution of effective orbitals for charge transport. According to the possible backbone conduction model,[46] the contorted "zigzag" backbone in Z-DNA is less favorable than the standard double helix in B-DNA, thereby lowering the conductance.

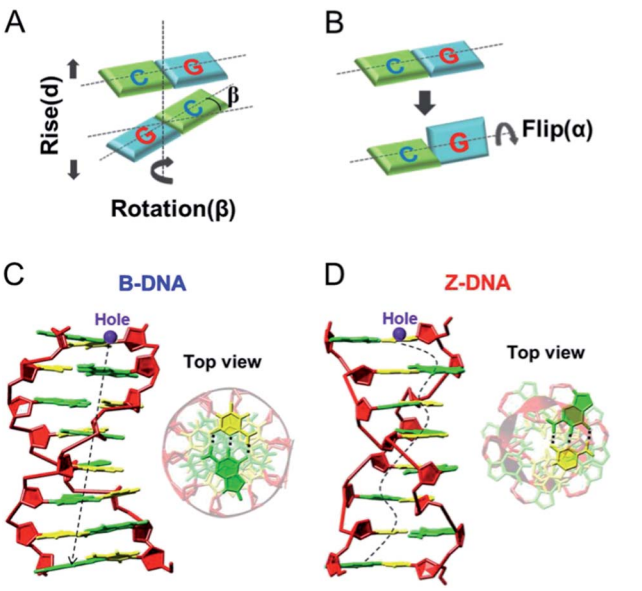

Fig. 6 (A) Schematics of relative changes between neighboring bps during the B–Z transition; (B) the schematic for guanine flipping. (C) and (D) show the structural side view and top view of B- and Z-DNA, respectively. In (C) and (D), the dashed lines demonstrates the intra-strand path for hole migration.

Apart from the impact of intrinsic structural change in DNA, the surrounding counter ions and water molecules also affect the charge transport process. It was reported that Mg^{2+} could bind to G and phosphate through its hydration shell.[47] Estimations based on our case show that there are on average 0.8 Mg^{2+} ions around a single DNA junction in 0.1 M $MgCl_2$ solution. But an average of 8.0 Mg^{2+} ions are available to bind to a single DNA molecule at 1 M, and even more ions are possible as the concentration increases (see Section S5†). It has to be noted that the dynamic movement of Mg^{2+} ions in solution greatly lowers the binding opportunity between the ions and DNA. Thus, it is plausible that higher concentrations (3 M, 4 M) are necessary to stabilize most DNA molecules in the Z-form.

Simulations[9] have suggested the delocalization of electron states induced by hydrated ions around DNA. Extra pathways for charge hopping could occur *via* ionization of phosphates and the doping of DNA grooves by Mg^{2+}, water states and base states.[48,49] Compared with the breaking of π–π orbital stacking, the influence of water and counter ions are presumed to be minor.

Transition degree (TD)

To quantify this DNA conformational change, we calculated the transition degree (TD), defined as the percentage of B-DNA which is converted to Z-DNA, as determined by our SHM conductance measurements. As an analogue to CD reported by others,[16] the key feature of our conductance histograms which allows the distinction between B- and Z-DNA is the two separate peaks. The SHM SPMBJ technique predicts that each plateau in every conductance trace is ideally equal in counts due to the constant duration, though the position changes. Therefore, each SHM conductance trace contributed equally to the final conductance histogram. Thus, the histogram is composed of a finite number of equally sized plateaus, the position of which is concentration dependent. By constructing histograms from two separate sets of traces, the transition degree was determined as SHM-TD $= A_Z/(A_Z + A_B)$, where A is the sum of counts beneath the first peak area in the SHM histograms. More calculation details can be found in Section S6 (see ESI†).

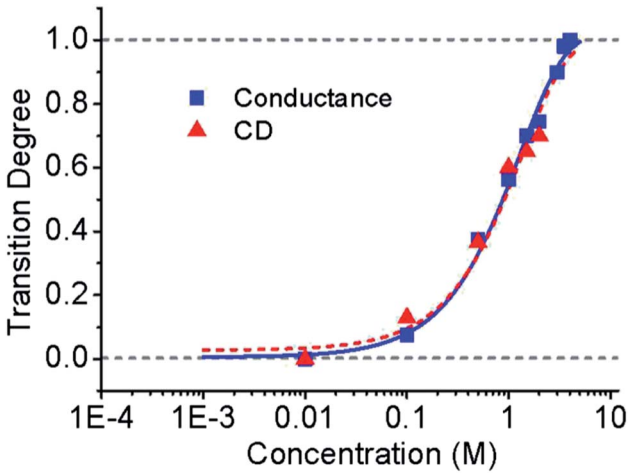

Fig. 7 TD *vs.* log $MgCl_2$ concentration. SHM-TD data points (■) and the corresponding Boltzmann fitting (solid curve). CD-TD data points (▲) and the corresponding fitting (dashed curve).

To accurately mark the transition midpoint, where 50% of B-DNA was converted into Z-DNA, it is important to first note that at low concentrations (0.1 M), past research has agreed the conformation is predominantly B-DNA. The Boltzmann fitting on the SHM-TD data (squares in Fig. 7) suggested the transition midpoint to be 0.93 M. This was larger than the previously reported value of around 0.66 M for indeterminately long strands of poly $d(GC)_m$ in $MgCl_2$ solution using CD.[16] But it matched well with the trend reported in the same paper, that the shorter the DNA length, the larger the concentration required to induce a 50% transition. Due to the sensitivity our electrical measurement has to high ionic concentration, we were unable to obtain meaningful results beyond 4 M. Similarly, the Boltzmann fitting suggests that the B–Z transition was saturated at around 4 M. Using the well-behaved part (0–2 M) of the CD results (triangles), we also plotted a CD-TD trend line (dashed curve). Boltzmann fitting was still suitable for estimating an entire transition line based on these CD results (ESI†). It suggested a transition midpoint (0.91 M) very close to the SHM-TD result. The SHM- and CD-TD trend lines overlap reasonably well.

Conclusions

Based on the SPMBJ technique, by increasing the concentration of $MgCl_2$ in the buffer solution, two different DNA conformations (B and Z) were distinguished exclusively by their difference in conductance due to the physical and electronic differences between the two conformations. Experimental results revealed that the increase of ionic concentration in a DNA sample solution induced a secondary structure transition of DNA molecules, and the conformational change reduced the DNA conductance by two orders of magnitude. Our technique successfully monitored changes in DNA conformation at a spatial and temporal resolution never before achieved, providing a powerful tool to explore some of the more confounding problems in molecular biology. In addition, using a SHM modification, our method offers an alternative way to build up transition trend lines between two DNA conformations, particularly when CD fails to work. This method is a general tool for studying transitions of other molecular properties associated with conductance differences.

Acknowledgements

This work was financially supported by National Science Foundation grants (ECCS 1231967, CBET 1139057).

Notes and references

1 C. Dekker and M. A. Ratner, *Phys. World*, 2001, **14**, 29–33.
2 Y. Ye, L. Chen, X. Z. Liu and U. J. Krull, *Anal. Chim. Acta*, 2006, **568**, 138–145.
3 J. C. Genereux and J. K. Barton, *Chem. Rev.*, 2010, **110**, 1642–1662.
4 S. S. Mallajosyula and S. K. Pati, *J. Phys. Chem. Lett.*, 2010, **1**, 1881–1894.
5 E. Braun, Y. Eichen, U. Sivan and G. Ben-Yoseph, *Nature*, 1998, **391**, 775–778.
6 H. W. Fink and C. Schonenberger, *Nature*, 1999, **398**, 407–410.
7 P. Tran, B. Alavi and G. Gruner, *Phys. Rev. Lett.*, 2000, **85**, 1564–1567.
8 A. Y. Kasumov, M. Kociak, S. Gueron, B. Reulet, V. T. Volkov, D. V. Klinov and H. Bouchiat, *Science*, 2001, **291**, 280–282.
9 R. N. Barnett, C. L. Cleveland, A. Joy, U. Landman and G. B. Schuster, *Science*, 2001, **294**, 567–571.
10 Y. A. Mantz, F. L. Gervasio, T. Laino and M. Parrinello, *Phys. Rev. Lett.*, 2007, **99**, 058104.
11 R. G. Endres, D. L. Cox and R. R. P. Singh, *Rev. Mod. Phys.*, 2004, **76**, 195–214.
12 A. Rich, *Gene*, 1993, **135**, 99–109.
13 P. Vasudevaraju, Bharathi, R. M. Garruto, K. Sambamurti and K. Rao, *Brain Res. Rev.*, 2008, **58**, 136–148.
14 H. Hamada, M. G. Petrino and T. Kakunaga, *Proc. Natl. Acad. Sci. U. S. A.*, 1982, **79**, 6465–6469.
15 A. Rich, A. Nordheim and A. Wang, *Annu. Rev. Biochem.*, 1984, **53**, 791–846.
16 F. M. Pohl and T. M. Jovin, *J. Mol. Biol.*, 1972, **67**, 375.
17 J. H. Van De Sande, L. P. McIntosh and T. M. Jovin, *EMBO J.*, 1982, **1**, 777–782.
18 A. Krzyzaniak, P. Salanski, J. Jurczak and J. Barciszewski, *FEBS Lett.*, 1991, **279**, 1–4.
19 V. I. Ivanov, L. E. Minchenk, E. E. Minyat, M. D. Frankkam and A. K. Schyolki, *J. Mol. Biol.*, 1974, **87**, 817–833.
20 J. Zheng, Z. Li, A. Wu and H. Zhou, *Biophys. Chem.*, 2003, **104**, 37–43.
21 B. Q. Xu, P. M. Zhang, X. L. Li and N. J. Tao, *Nano Lett.*, 2004, **4**, 1105–1108.
22 K. Siriwong and A. A. Voityuk, *J. Phys. Chem. B*, 2008, **112**, 8181–8187.
23 S. S. Mallajosyula, A. Gupta and S. K. Pati, *J. Phys. Chem. A*, 2009, **113**, 3955–3962.

24 D. R. Latulippe and A. L. Zydney, *Biotechnol. Bioeng.*, 2008, **99**, 390–398.
25 F. L. Gervasio, P. Carloni and M. Parrinello, *Phys. Rev. Lett.*, 2002, **89**, 108102.
26 R. Gutierrez, S. Mandal and G. Cuniberti, *Nano Lett.*, 2005, **5**, 1093–1097.
27 B. Q. Xu and N. J. Tao, *Science*, 2003, **301**, 1221–1223.
28 J. Zhou, F. Chen and B. Xu, *J. Am. Chem. Soc.*, 2009, **131**, 10439–10446.
29 J. Hihath, B. Xu, P. Zhang and N. Tao, *Proc. Natl. Acad. Sci. U. S. A.*, 2005, **102**, 16979–16983.
30 S. Lindsay, *Faraday Discuss.*, 2006, **131**, 403–409.
31 C. Li, I. Pobelov, T. Wandlowski, A. Bagrets, A. Arnold and F. Evers, *J. Am. Chem. Soc.*, 2008, **130**, 318–326.
32 E. Wierzbinski, R. Venkatramani, K. L. Davis, S. Bezer, J. Kong, Y. Xing, E. Borguet, C. Achim, D. N. Beratan and D. H. Waldeck, *ACS Nano*, 2013, **7**, 5391–5401.
33 H. van Zalinge, D. J. Schiffrin, A. D. Bates, W. Haiss, J. Ulstrup and R. J. Nichols, *ChemPhysChem*, 2006, **7**, 94–98.
34 S. Brahms and J. G. Brahms, *Nucleic Acids Res.*, 1990, **18**, 1559–1564.
35 E. Segal and J. Widom, *Curr. Opin. Struct. Biol.*, 2009, **19**, 65–71.
36 J. H. Vandesande and T. M. Jovin, *EMBO J.*, 1982, **1**, 115–120.
37 T. Miyahara, H. Nakatsuji and H. Sugiyama, *J. Phys. Chem. A*, 2013, **117**, 42–55.
38 P. Varnai and Y. Timsit, *Nucleic Acids Res.*, 2010, **38**, 4163–4172.
39 E. Hamori and T. M. Jovin, *Biophys. Chem.*, 1987, **26**, 375–383.
40 F. J. Ramirez, T. J. Thomas, T. Antony, J. Ruiz-Chica and T. Thomas, *Biopolymers*, 2002, **65**, 148–157.
41 S. K. Zavriev, L. E. Minchenkova, M. Vorlickova, A. M. Kolchinsky, M. V. Volkenstein and V. I. Ivanov, *Biochim. Biophys. Acta, Nucleic Acids Protein Synth.*, 1979, **564**, 212–224.
42 G. S. Kumar and M. Maiti, *J. Biomol. Struct. Dyn.*, 1994, **12**, 183–201.
43 G. J. Puppels, C. Otto, J. Greve, M. Robertnicoud, D. J. Arndtjovin and T. M. Jovin, *Biochemistry*, 1994, **33**, 3386–3395.
44 C. R. Treadway, M. G. Hill and J. K. Barton, *Chem. Phys.*, 2002, **281**, 409–428.
45 A. Hubsch, R. G. Endres, D. L. Cox and R. R. P. Singh, *Phys. Rev. Lett.*, 2005, **94**, 178102.
46 H. Ikeura-Sekiguchi and T. Sekiguchi, *Phys. Rev. Lett.*, 2007, **99**, 228102.
47 R. V. Gessner, G. J. Quigley, A. H. J. Wang, G. A. Vandermarel, J. H. Vanboom and A. Rich, *Biochemistry*, 1985, **24**, 237–240.
48 V. V. Zakjevskii, S. J. King, O. Dolgounitcheva, V. G. Zakrzewski and J. V. Ortiz, *J. Am. Chem. Soc.*, 2006, **128**, 13350–13351.
49 J. M. Soler, E. Artacho, J. D. Gale, A. Garcia, J. Junquera, P. Ordejon and D. Sanchez-Portal, *J. Phys.: Condens. Matter*, 2002, **14**, 2745–2779.